Geophysical Research Letters

RESEARCH LETTER
10.1029/2021GL093882

Key Points:

- Subsurface brines can deposit significant potassium in volcanic rocks while preserving original textures
- Spectral signatures of K-metasomatism include K-feldspar and illite
- Felsic compositions on Mars might occur because of low-temperate alteration by subsurface brines

Supporting Information:

Supporting Information may be found in the online version of this article.

Correspondence to:

J. R. Michalski,
jmichal@hku.hk

Citation:

Michalski, J. R., Niles, P. B., Glotch, T. D., & Cuadros, J. (2021). Infrared spectral evidence for K-metasomatism of volcanic rocks on Mars. *Geophysical Research Letters*, *48*, e2021GL093882. https://doi.org/10.1029/2021GL093882

Received 10 DEC 2020
Accepted 23 APR 2021

Infrared Spectral Evidence for K-Metasomatism of Volcanic Rocks on Mars

Joseph R. Michalski[1,2], Paul B. Niles[3], Timothy D. Glotch[4], and Javier Cuadros[5]

[1]Division of Earth & Planetary Science, University of Hong Kong, Hong Kong, China, [2]Laboratory for Space Research, University of Hong Kong, Hong Kong, China, [3]NASA Johnson Space Center, Houston, TX, USA, [4]Stony Brook University, Stony Brook, NY, USA, [5]Natural History Museum, London, UK

Abstract Potassium metasomatism is a common geologic process occurring in a range of environments on Earth. K-metasomatism can dramatically change the chemistry of large volumes of crust resulting in formation of abundant K-rich feldspar while preserving original rock textures. Remote sensing of Mars has revealed the presence of rare but striking felspar-rich terrains as well as K-rich phyllosilicates such as illite or muscovite. Furthermore, the Curiosity Rover has detected evidence for K-enrichment in rocks at Gale Crater. In this study, we use spectroscopic and remote sensing analyses of K-metasomatized rocks on Earth as a comparison to K-rich and/or possible granitic rocks on Mars. The results suggest that evidence for K-feldspar rich, quartz-bearing, and illite-bearing rocks on Mars is consistent with K-metasomatism. K-rich rocks in Gale Crater have themselves likely not been metasomatized, but the abundant feldspar within them might have been derived from metasomatized crust.

Plain Language Summary Mars is a volcanic planet with a surface dominated by basalt and sedimentary rocks derived from basalt, similar to oceanic crust on Earth (though Mars' crust is thicker). For decades, Mars has been considered a "one plate planet" where plate tectonics never occurred and where continental type rocks never formed. Recent observations have, however, revealed enticing evidence that felsic "continental type" rocks containing K-feldspar and quartz are present. Such rock units were recognized in Gale Crater based on their high potassium abundances. Granite-type rocks detected from orbit using infrared data would also presumably be rich in potassium. However, rocks of the same composition can be made through aqueous alteration rather than from magma in the crust. This study shows a striking example of potassium enrichment and mineralogical changes in basaltic rocks on Earth caused entirely by low-temperature hydrothermal brine in the crust. We use analogous remote sensing measurements to study these potassic rocks on Earth and compare the results to Mars. It appears that at least some of the felsic rock compositions on Mars were caused by metasomatism.

1. Introduction

Potassium is an incompatible lithophile element that is mobilized and concentrated by aqueous processes under a range of conditions. Its concentration and distribution on Mars therefore contain valuable information about past igneous and alteration processes that have affected the crust. Gamma Ray Spectroscopy (GRS) measurements of Mars from orbit indicate that the crust is generally potassium-poor, with atomic K concentrations of ~0.2–0.6 (Boynton et al., 2007). But variations in K-concentration and K/Th ratios speak to possible igneous evolution or limited aqueous alteration at the broad spatial scales of the Mars Odyssey GRS measurements (Karunatillake et al., 2009; Taylor et al., 2007).

Orbital infrared remote sensing data provide additional perspective on the idea of igneous evolution and K-enrichment at higher spatial resolution than is possible with GRS data (Christensen et al., 2005; Rogers et al., 2007). Thermal infrared emission data from the 2001 Mars Odyssey Thermal Emission Imaging System (THEMIS) have revealed rock compositions similar to granite exhumed from the subsurface in some ancient terrains (Figure 1; Bandfield, 2006). THEMIS data combined with Mars Global Surveyor (MGS) Thermal Emission Spectrometer (TES) data suggest that the rocks are composed of K-feldspar and quartz, along with other phases (Bandfield et al., 2004). These detections are categorically related to, but distinct from, anorthite-bearing rocks detected with the Mars Reconnaissance Orbiter (MRO) Compact Reconnaissance Imaging Spectrometer for Mars (CRISM; Carter & Poulet, 2013; Wray et al., 2013). The units

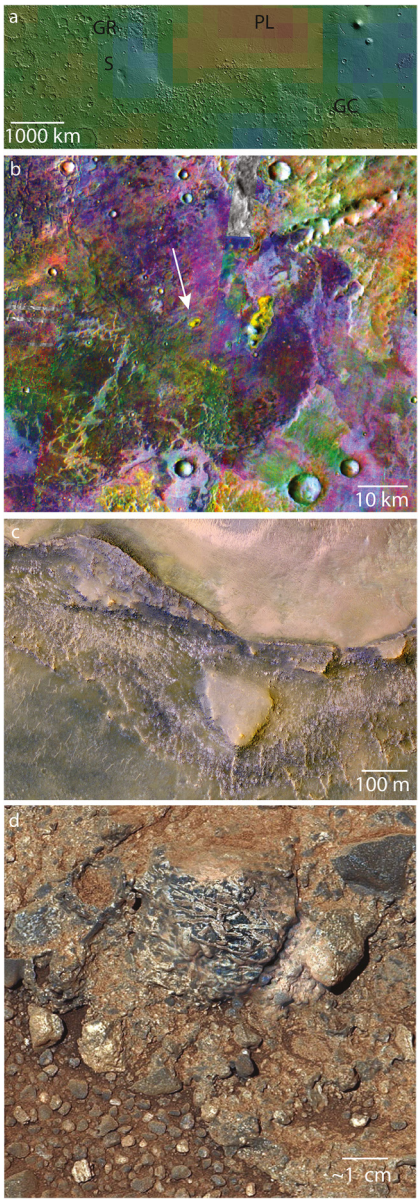

Figure 1. GRS K-abundance is shown in (a) where blue tones correspond to 0.2 atomic wt% K and red corresponds to 0.5%. A THEMIS DCS (bands 8,7,5 as R, G, B) is shown in (b) for the area of granitoid-type compositions detected by Bandfield (2006) (20.45N, 62.82E). Yellow corresponds to felsic compositions in the decorrelation stretch (DCS) image. A white arrow points to the location of the HiRISE false color IRB image shown in (c), which reveals meter-scale layering in the felsic material. A Mastcam image of potential continental-type crust showing light-toned laths interpreted as feldspar and known to contain high-potassium values form ChemCam data is shown in (d). HiRISE image is ESP_016048_2005 and THEMIS mosaic includes images I01677033, I06489025, and I43165002. Mastcam 100 image of rock target Harrison.

identified by CRISM have been shown to be inconsistent with highly felsic rocks, although anorthosite compositions are permissible (Rogers & Nekvasil, 2015). Some key differences between the detections made using THEMIS and TES thermal infrared data versus CRISM near infrared data is that the thermal IR data suggest the presence of K-feldspar and quartz, and the CRISM data suggest Ca/Fe-rich plagioclase (and the near infrared is not sensitive to quartz or K-feldspar).

A complication arises, however, in considering the effects of alteration on igneous interpretations of infrared data. CRISM-based near infrared observations of the THEMIS granitoid-type rocks show that they contain a suite of alteration phases such as amorphous silica and Al-rich clay minerals (Smith & Bandfield, 2012). These observations differ from the infrared signature of weathered, natural surfaces of granitic rocks on Earth (Michalski et al., 2004) and are instead suggestive of hydrothermal or diagenetic processes. The Martian granitoid-type rocks are also layered, which suggests they might be altered ash deposits. These rock compositions might indicate K-enrichment in the form of secondary feldspar and Al-clays such as illite or muscovite.

In the same ancient terrain where the granitoid-type compositions occur, CRISM data have revealed the presence of K-rich phyllosilicates such as illite or muscovite (the two are not readily distinguishable with CRISM data) in rocks exhumed from the subsurface by impact craters (Ehlmann et al., 2009). The mineralogy and geologic context of these rocks points to the origin of K-rich rocks in some cases by diagenetic and hydrothermal processes (Ehlmann et al., 2011). It bears noting here that the anorthite-rich rocks detected elsewhere on Mars using CRISM data also contain spectral absorptions near 2.2 μm indicating the likely presence of Al-phyllosilicates in many of those deposits (Carter & Poulet, 2013; Wray et al., 2013).

Surface operations by the Curiosity Rover have shown K-enrichments within multiple rock types in Gale Crater. Measurements by the Alpha Particle X-ray Spectrometer (APXS) and Chemistry Camera (ChemCam) and Mast Camera (Mastcam) show that some large boulders with plutonic textures (e.g., plagioclase laths) have elevated K-content (Figure 1d). These rocks have been interpreted as evidence for distal "continental" type crustal units near the northern rim of Gale Crater, to the north of the landing site (Sautter et al., 2015). Some sedimentary units Gale Crater represent the most K-rich rocks identified on Mars to date (Le Deit et al., 2016; Thompson et al., 2016). Chemical associations in the analyses published to date suggest that the K resides in detrital K-feldspar such as sanidine or orthoclase, rather than secondary minerals such as illite (Treiman et al., 2016).

Although the surface of Mars appears to be generally K-poor from a GRS perspective, regional and local remote sensing and rover results demonstrate that potassic sedimentary and igneous rocks are part of the Martian geological puzzle. One possible explanation is that igneous evolution has produced K-rich rocks through fractional crystallization of magmas from a mantle that is K-rich compared to that of Earth (Stolper et al., 2013). Another possibility is that local or regional-scale K-metasomatism has occurred on Mars, causing K-enrichment in igneous rocks by low-temperature brines at the surface or in the subsurface. This study explores the second hypothesis, K-metasomatism, through investigation of a case of brine alteration of mafic volcanic rocks that occurred in western Arizona, USA.

2. A Terrestrial Analog for K-Metasomatism of Basalt on Mars

During the Miocene, tectonically controlled, arid basins existed throughout the southwestern USA (Spencer et al., 1995). Saline lakes formed in arid tectonic basins. Downwelling and laterally migrating low-temperature hydrothermal brine in the subsurface produced widespread K-metasomatism of volcanic rocks throughout the region (Chapin & Lindley, 1985; Ennis et al., 2000). An unusual and interesting aspect of K-metasomatism is that it is only recognizable from chemical measurements, typically in a laboratory setting. Rock textures and color are often completely preserved, despite significant changes in geochemistry.

In the Buckskin Mountains in western Arizona, Miocene basalt, tuff and volcaniclastic breccias have been K-metasomatized. Previous work focused on the mineralogy and geochemistry of these rocks in the Swansea area of western Arizona with regard to geologic history and economic geology (Michalski et al., 2007). Those results show that the metasomatized basalts have K_2O abundances 5.4%–11.8% and K/Na ratios of 104–526. The altered pyroclastics have K_2O values of 8.8%–9.4% and K/Na ratios of 31–44. XRD results show that the original mineralogy of the volcanic rocks has been completely changed to a simple assemblage of K-feldspar, illite and minor hematite and quartz (Michalski et al., 2007). An atypical aspect of the alteration at Swansea is that the early phase of K-metasomatism was followed by a subsequent phase of carbonation, which unlike the K-metasomatism, did disrupt the volcanic textures. Though the carbonate replacements at Swansea have no direct link to K-enrichment, this character of the rocks is also of interest for better understanding carbonated rocks exhumed from Martian subsurface (Michalski & Niles, 2010; Wray et al., 2016). This study applies new remote sensing and spectroscopic data of K-metasomatized rocks from Swansea in order to better understand remote sensing of K-feldspar and illite-bearing terrains on Mars, and K-enrichments detected geochemically within Gale Crater.

3. Laboratory Spectroscopy of Metasomatized Volcanic Rocks

Micro-infrared spectroscopic mapping was carried out in the Planetary Spectroscopy and Mineralogy Laboratory (PSML) at the University of Hong Kong. Reflectance spectra were collected from 650 to 4,000 cm^{-1} on a Nicolet Continuum Infrared microscope with 8 cm^{-1} spectral sampling, using a gold reference standard. Using a 30 μm step size (spatial sampling) and 8 scan integration, hyperspectral maps of ~8 × 8 mm areas of polished thin sections were collected over ~20 h with a nitrogen-cooled mercury cadmium telluride detector. Figure 2a shows a field photo of the outcrop of altered basalt in the Swansea area (34.16°N, 113.87°W), and micro-infrared reflectance images of basalt and pyroclastic materials.

Blue areas in Figure 2b correspond to carbonate replacements that are younger than the K-metasomatism. The orange-yellow silicate pattern in Figure 2b reflects the original volcanic texture of the rock. Here, the original 100–300 μm-long plagioclase laths (yellow) are observed within an orange groundmass of what was previously glass, amphibole and pyroxene. However, extracted infrared spectra from each of these phases shows that the plagioclase has been entirely converted to K-feldspar and the ferromagesian phases have been entirely replaced by illite. Later carbonate replacements are nearly pure calcite with accessory hematite.

The brecciated pyroclastic unit shows similar, but not identical patterns. Fragments of basaltic ash have been replaced by K-feldspar and illite (Figures 2d and 2e). The altered basalt is physically mixed with fragmented quartz and carbonate. Note that hematite has no spectral features in this part of the thermal infrared spectral range and cannot be detected or mapped uniquely.

Visible/near-infrared reflectance spectra of rock powders and chips were acquired at the PSML from 550 to 2,500 nm using a Spectralon reflectance standard by integrating 60 scans over a period of ~1 min from a spot size of ~3 mm^2 in a Praying Mantis diffuse reflectance chamber attached to a Nicolet iS50 interferometer. Figure 3 shows reflectance spectra of a natural surface of altered basalt as well as the same unit powdered to <2 μm. Note that the rock chip shows a strong blue-slope, but also exhibits OH and HOH absorptions at ~1,410 and ~1,910 nm, respectively. These features and an Al-OH absorption at 2,214 nm trace the occurrence of illite clay. However, typical illite (shown in green in Figure 3a) is relatively Fe-poor and the illite in the altered basalt from Swansea contains 4–5 times more Fe (Michalski et al., 2007). A strong,

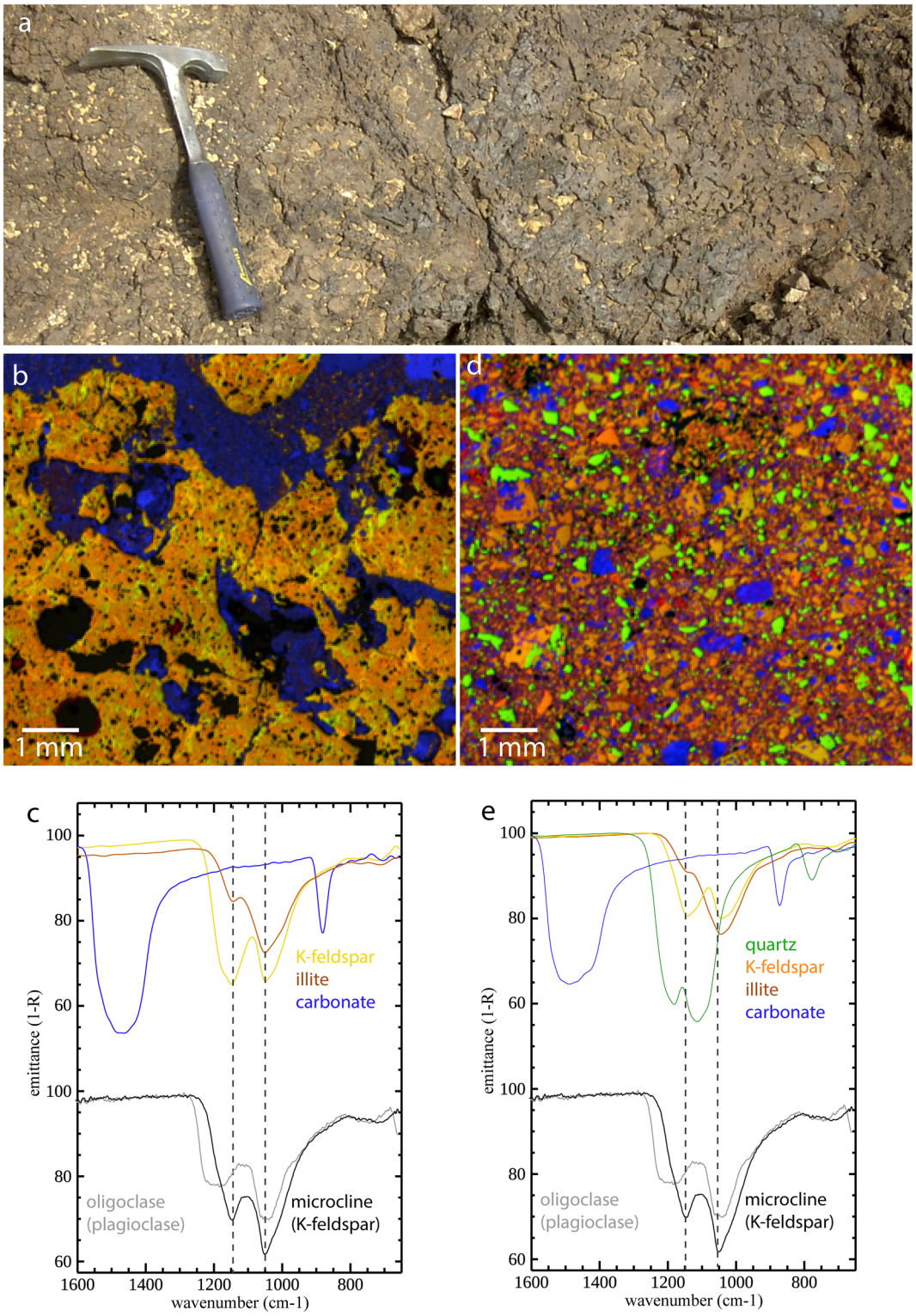

Figure 2. A field photo of altered basalt in the Swansea, Arizona area is shown in (a). Micro-infrared reflectance maps of thin sections are shown for metasomatized basalt (b) and metasomatized ash (c). The corresponding emittance spectra of each image are shown below, (d) shows emittance spectra (1-reflectance) of spectra from the metasomatized basalt and (e) shows emittance spectra from the metasomatized ash. The spot size of each spectrum is approximately 30 micrometers across. Colors of spectra in (c and e) correspond to colors observed in the corresponding images above each plot. Emittance spectra are measured reflectance converted using Kirkoff's Law (1-reflectance) top emissivity.

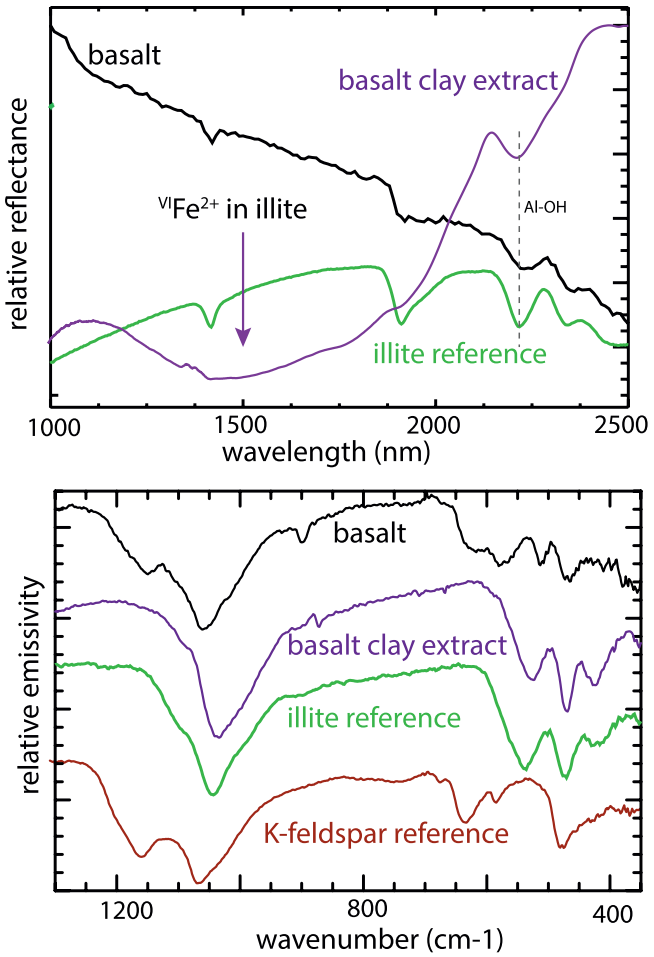

Figure 3. VNIR data for the metasomatized basalt measured as a rock chip compared to measurement of the <2 μm size fraction ("basalt clay extract") measured as a powder show the different spectral character of the two materials and illustrate key properties of the illitic clay component relative to other illite standards such as IMt-1 ("illite reference spectrum") (a). This material has a strong absorption related to Al-OH at 2200 nm, as do other illites. But, some octahedral (VI-coordinated) Fe^{2+} is present, resulting in a strong, broad absorption from ~1100 to 1800 nm. Thermal infrared emission spectra of the basalt chip versus clay extract are show in (b). The emission spectrum of Imt-1 and a K-feldspar (orthoclase) reference standard are shown.

broad absorption between 1,000 and 2,000 nm in Swansea illite indicates that Fe^{2+} occurs in 6-coordinated octahedral sites (Chemtob et al., 2015).

Thermal infrared emission spectra were collected from 200 to 2,000 cm^{-1} at the Arizona State University Mars Space Flight Facility using procedures described previously (Ruff et al., 1997). Both basalt whole-rock samples and 1 cm-diameter pellets composed of the <2 μm (clay-size) fraction were measured (Figure 3b). The whole rock samples contain spectral absorptions at ~1,160, 1,060, 640, and 460 cm^{-1} indicative of K-feldspar and absorptions at 460, 540, and 1,065 cm^{-1} indicative of illite. Note that the Si-O-metal absorption in illite is shifted to longer wavenumber in this illite compared to the IMt-1 standard because of the substation of larger Fe^{2+} for Al^{3+} in the octahedral sheet, creating longer bond distances and lower frequency vibrations (Michalski et al., 2006).

4. Remote Sensing of K-Metasomatized Rocks on Earth

High spatial resolution multispectral remote sensing analysis was carried out using data from the Worldview-3 (WV3) satellite. WV3 provides panchromatic data at ~30 cm/pixel spatial resolution, 8 spectral channels in the visible-near infrared (VNIR; ~400–1,000 nm) range at ~1.2 m/pixel, and 8 spectral channels in the short wave infrared (SWIR; ~1,200–2,400 nm) at 3.7 m/pixel (see supplementary material for details). Data were obtained from the vendor (Satellite Imaging Corporation) in calibrated, geo-rectified format. No atmospheric corrections were applied to any of the wavelengths because such corrections are not necessary for the VNIR range and because only band ratios and relative spectral index measurements were used for the SWIR data (e.g., Mars, 2018).

VNIR data displayed in near true color show colorful sedimentary, volcanic, and plutonic rocks within a shallow SW-NE trending valley in the Swansea area (Figure 4a). In fact, the valley is a shallow synform bounded by similarly trending mylonitic crystalline rock to the north and south. All of the sedimentary, volcanic and plutonic rocks in the valley represent the upper plate of the Buckskin-Rawhide detachment fault (BRDF), which has significant extension in the Miocene.

A SWIR principal components analysis (PCA) image emphasizes compositional differences among units. Principle components 4, 3, and 2 are displayed as R, G, and B, respectively (Figure 4b). The geological units (defined by white dotted lines) shown in Figure 4b are based on mapping carried out by Spencer and Reynolds 1986 but simplified here for clarity. The most important units to note are units "MB," which is the K-metasomatized basalt, "MBa," which is alluvium derived from erosion of unit MB, and "MBb," which is metasomatized basalt-pyroclastic breccia. Other units include: "mc" is mylonitic crystalline basement rock; "XTi" is Jurassic-Tertiary intrusive meta-granite, "MPs" corresponds to Mesozoic and Paleozoic metasediments, mostly dolostone-marble with some sandstone; "Tb" is the lower breccia unit; In panel "d," the MBa unit derived from erosion of the metasomatized bedrock is marked by arrows.

A band ratio of WV3 SWIR data was used to delineate and map clay minerals according to the following formula: (R_{2260}/R_{2205}) * (R_{2165}/R_{1730}) where the subscript corresponds to the wavelength position in nm of WV3 bands 4, 5, 6, and 7 (Figure 4c). This spectral index measures the occurrence of the Al-OH absorption in the numerator and the presence of an Fe^{2+}-related spectral slope in the denominator, resulting in high values for surfaces that have both of those features. The spectral index map illustrates how illite is associated with the occurrence of unit MB (metasomatized basalt) and MBb (metasomatized basaltic breccia).

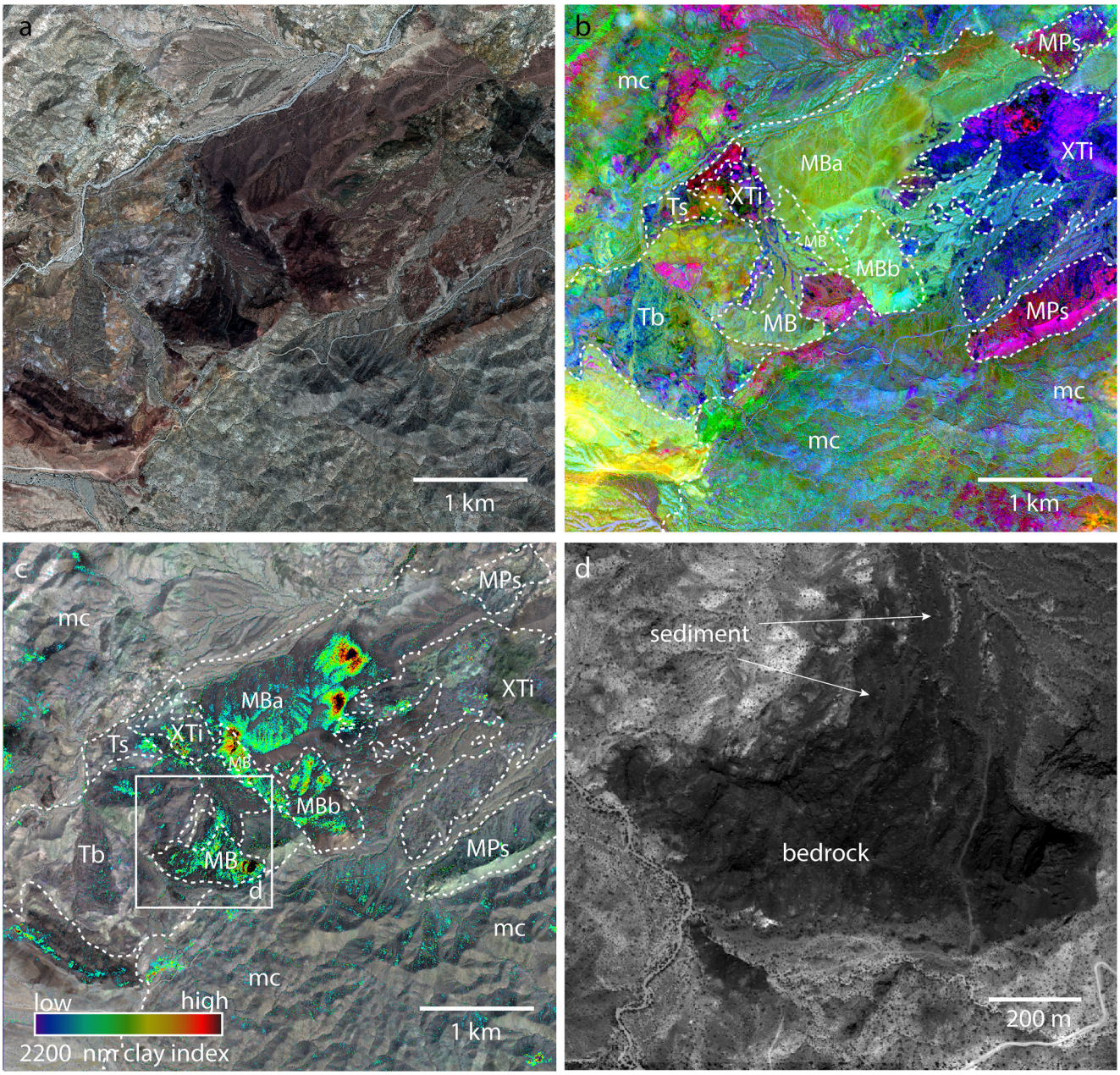

Figure 4. Worldview VNIR color data (bands 5,3,2 as RGB) of the Swansea, Arizona area (113.9 W, 34.2 N) are shown in (a). Worldview 3 SWIR PCA image where PCA bands 4,3,2 are displayed as RGB are shown in (b). The WV3 clay index (5 over 6 over 7) are shown in (c). Panchromatic WV data are shown in (d), illustrating the exposure of bedrock and sediments derived from the bedrock.

Furthermore, the sediments derived from these two units (MBa), which are transported toward the north and northeast, carry the spectral signature of the alteration as detected by remote sensing instruments.

Thermal infrared emissivity data from the Advanced Spaceborne Thermal Emission and Reflectance Radiometer (ASTER) show a different perspective on the K-metasomatized rocks. ASTER emissivity data were obtained as atmospherically corrected, calibrated emissivity. Figure 5 shows a false color (pan-sharpened) emissivity image of the Buckskin Mountains and the extracted emission spectrum of the metasomatized basalt unit. At multispectral resolution (5 bands, in the case of ASTER), the spectral shape of K-metasomatized basalt is strikingly similar to alkali granite measured in the laboratory (Guha & Vinod Kumar, 2016).

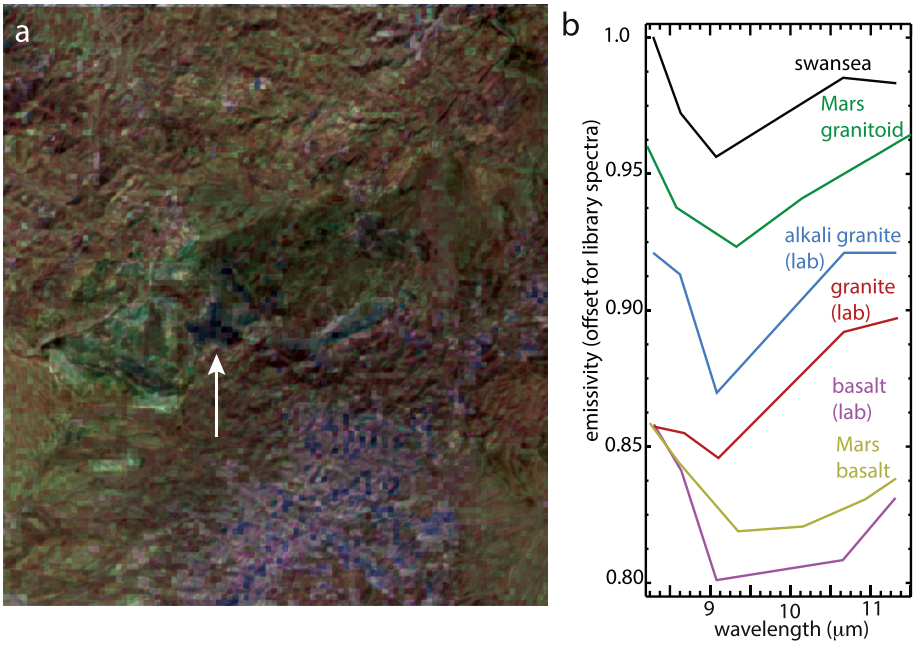

Figure 5. An ASTER pan-sharpened emissivity image is shown in (a). The extracted emissivity spectrum of the K-metasomatized basalt unit is shown in (b) (labeled "Swansea"). A THEMIS emissivity spectrum of the granitoid-type materials from Bandfield (2006) is shown in green. Note this spectrum corresponds to the material in Figures 1b and 1c. The remote sensing spectra are compared to laboratory spectra of granite (Michalski et al., 2004), alkali granite and basalt resampled to ASTER spectral resolution. A THEMIS spectrum of Martian basalt is shown for comparison (yellow).

THEMIS emissivity extracted from granitoid-type compositions on Mars (Bandfield, 2006) are compared to the ASTER emissivity data of K-metasomatized basalt and lab spectra of igneous rocks in Figure 5. At multispectral resolution, K-feldspar-rich, illite-bearing K-metasomatized volcanic rocks are similar to granitoid-type compositions detected on Mars. Metasomatic alteration by low-temperature hydrothermal brines could be a viable mechanism to produce feldspar-rich, clay-bearing rocks detected on Mars by infrared techniques (Figure 5).

5. Summary and Conclusions for Mars

Swansea, Arizona contains a striking example of K-metasomatized volcanic rocks, but the processes that operated in that area are not geologically uncommon. Rift basins (Roddy et al., 1988), calderas (Nusbaum & Grant, 1987), seafloor sediments (Rouchon & Orberger, 2008) and paleosols (Novoselov & de Souza Filho, 2015) all display evidence for K-metasomatism. A similar process would likely have operated on Mars as well given that surface and shallow subsurface has at times likely contained abundant reactive, glassy rocks (Bandfield et al., 2013; Horgan & Bell, 2012) to liberate cations, concentrated, mobile brines to transport those cations (Knauth & Burt, 2002), and reactive rocks susceptible to metasomatism (see supporting information). Gradual extraction of cations from the fluid including Mg^{2+}, Ca^{2+} during crystallization of sulfates or carbonates in the crust would further serve to concentrate K^{+}. But even if Na^{+} is more abundant than K^{+} in a hydrothermal fluid, K-feldspar can form because it is more stable in low-temperature hydrothermal conditions (Chapin & Lindley, 1985).

This study describes chemical, spectroscopic and remote sensing signatures of K-metasomatized rocks on Earth, providing insight into their potential signatures on Mars. Multispectral thermal infrared remote sensing shows that K-metasomatized basalts have similar spectral character to granite and alkali granite. The K-rich clay illite is generally common in K-metasomatism and Fe-bearing illite is a key component of the alteration assemblage at Swansea. The spectroscopic and remote sensing signatures of K-metasomatism demonstrated at Swansea are in many ways similar to infrared observations of Mars showing granitoid-like,

Al-clay-bearing rocks in the Noachian Crust (Figure 1) or illite-bearing crust exhumed by meteor impact. Given that the granitoid-type compositions actually correspond to layered rocks (Figure 1b), we propose that these materials might represent mafic volcanic materials (e.g., pyroclastics) that have been metasomatized by crustal fluids.

K-enrichment detected chemically at Gale Crater is more complicated. The sedimentary rocks containing the K-rich clasts have likely not been metasomatized because those rocks contain abundant Ca, Na, and Mg, all of which are strongly depleted by K-metasomatism. But, the K-enrichment at Gale Crater likely reflects detrital K-feldspar in the rocks. It is therefore unknown if the K-feldspar was eroded from a felsic volcanic or granitic protolith, though in cases where sanidine is the carrier of K, primary volcanic processes should be expected. The occurrence of K-feldspars such as microcline and orthoclase, be they in igneous rocks or as detritus in sedimentary rocks could have ultimately formed in hydrothermal settings in mafic volcanic terrain on Mars and are not necessarily indicators of felsic crust.

Data Availability Statement

JMARS software used in study is available through Arizona State University at https://jmars.asu.edu/. Mars remote sensing data are all available through the Planetary Data System. All data used in this study are available in the NASA Planetary Data System (pds.jpl.nasa.gov). Mars Odyssey Gamma Ray Spectrometer data are available at https://pds-geosciences.wustl.edu/missions/odyssey/grs.html. Mars Odyssey THEMIS data are available at: https://pds-geosciences.wustl.edu/missions/odyssey/themis.html. Mars Curiosity Rover Mastcam data are available at: https://pds-geosciences.wustl.edu/missions/msl/. Worldview 3 remote sensing data are available at: https://zenodo.org/record/4643735#.YGGhJeYRVp8. Micro-infrared data are available at: https://zenodo.org/record/4643764#.YGGlBuYRVp8. ASTER data are available at: https://search.earthdata.nasa.gov/search.

Acknowledgments
J. Michalski was funded by the Hong Kong Research Grants Council General Research Fund (17307417).

References

Bandfield, J. L. (2006). Extended surface exposures of granitoid compositions in Syrtis Major, Mars. *Geophysical Research Letters*, *33*(6), L06203. https://doi.org/10.1029/2005gl025559

Bandfield, J. L., Edwards, C. S., Montgomery, D. R., & Brand, B. D. (2013). The dual nature of the Martian crust: Young lavas and old clastic materials. *Icarus*, *222*(1), 188–199. https://doi.org/10.1016/J.Icarus.2012.10.023

Bandfield, J. L., Hamilton, V. E., Christensen, P. R., & McSween, H. Y. (2004). Identification of quartzofeldspathic materials on Mars. *Journal of Geophysical Research*, *109*(E10), E10009. https://doi.org/10.1029/2004je002290

Boynton, W. V., Taylor, G. J., Evans, L. G., Reedy, R. C., Starr, R., Janes, D. M., et al. (2007). Concentration of H, Si, Cl, K, Fe, and Th in the low- and mid-latitude regions of Mars. *Journal of Geophysical Research*, *112*(E12), 1–15. https://doi.org/10.1029/2007je002887

Carter, J., & Poulet, F. (2013). Ancient plutonic processes on Mars inferred from the detection of possible anorthositic terrains. *Nature Geoscience*, *6*(12), 1008–1012. https://doi.org/10.1038/Ngeo1995

Chapin, C. E., & Lindley, J. I. (1985). *Potassium metasomatism of volcanic and sedimentary rocks in rift basins, calderas and detachment terranes*. In Heat and detachment in crustal extension on continents and planets.

Chemtob, S. M., Nickerson, R. D., Morris, R. V., Agresti, D. G., & Catalano, J. G. (2015). Synthesis and structural characterization of ferrous trioctahedral smectites: Implications for clay mineral genesis and detectability on Mars. *Journal of Geophysical Research: Planets*, *120*, 1119–1140. https://doi.org/10.1002/2014JE004763

Christensen, P. R., McSween, H. Y., Bandfield, J. L., Ruff, S. W., Rogers, A. D., Hamilton, V. E., et al. (2005). Evidence for magmatic evolution and diversity on Mars from infrared observations. *Nature*, *436*(7050), 504–509. https://doi.org/10.1038/Nature03639

Ehlmann, B. L., Mustard, J. F., Clark, R. N., Swayze, G. A., & Murchie, S. L. (2011). Evidence for low-grade metamorphism, hydrothermal alteration, and diagenesis on mars from phyllosilicate mineral assemblages. *Clays and Clay Minerals*, *59*(4), 359–377. https://doi.org/10.1346/CCMN.2011.0590402

Ehlmann, B. L., Mustard, J. F., Swayze, G. A., Clark, R. N., Bishop, J. L., Poulet, F., et al. (2009). Identification of hydrated silicate minerals on Mars using MRO-CRISM: Geologic context near Nili Fossae and implications for aqueous alteration. *Journal of Geophysical Research*, *114*, E00d08. https://doi.org/10.1029/2009je003339

Ennis, D. J., Dunbar, N. W., Campbell, A. R., & Chapin, C. E. (2000). The effects of K-metasomatism on the mineralogy and geochemistry of silicic ignimbrites near Socorro, New Mexico. *Chemical Geology*, *164*, 285–312. https://doi.org/10.1016/S0009-2541(99)00223-5

Guha, A., & K., V. K. (2016). New ASTER derived thermal indices to delineate mineralogy of different granitoids of an Archaean Craton and analysis of their potentials with reference to Ninomiya's indices for delineating quartz and mafic minerals of granitoids-An analysis in Dharwar Craton, India. *Ore Geology Reviews*, *74*, 76–87. https://doi.org/10.1016/j.oregeorev.2015.10.033

Horgan, B., & Bell, III, J. F. (2012). Widespread weathered glass on the surface of Mars. *Geology*, *40*, 391–394. https://doi.org/10.1130/G32755.1

Karunatillake, S., Wray, J. J., Squyres, S. W., Taylor, G. J., Gasnault, O., McLennan, S. M., et al. (2009). Chemically striking regions on Mars and Stealth revisited. *Journal of Geophysical Research*, *114*(E12), 1–35. https://doi.org/10.1029/2008je003303

Knauth, L., & Burt, D. M. (2002). Eutectic brines on Mars: Origin and possible relation to young seepage features. *Icarus*, *158*(1), 267–271. https://doi.org/10.1006/icar.2002.6866

Le Deit, L., Mangold, N., Forni, O., Cousin, A., Lasue, J., Schröder, S., et al. (2016). The potassic sedimentary rocks in Gale Crater, Mars, as seen by ChemCam on boardCuriosity. *Journal of Geophysical Research: Planets*, *121*, 784–804. https://doi.org/10.1002/2015JE004987

Mars, J. C. (2018). Mineral and lithologic mapping capability of worldview 3 data at Mountain Pass, California, using true- and false-color composite images, band ratios, and logical operator algorithms. *Economic Geology*, *113*, 1587–1601. https://doi.org/10.5382/econgeo.2018.4604

Michalski, J. R., Kraft, M. D., Sharp, T. G., Williams, L. B., & Christensen, P. R. (2006). Emission spectroscopy of clay minerals and evidence for poorly crystalline aluminosilicates on Mars from thermal emission spectrometer data. *Journal of Geophysical Research*, *111*(3). https://doi.org/10.1029/2005JE002438

Michalski, J. R., & Niles, P. B. (2010). Deep crustal carbonate rocks exposed by meteor impact on Mars. *Nature Geoscience*, *3*(11), 751–755. https://doi.org/10.1038/ngeo971

Michalski, J. R., Reynolds, S. J., Niles, P. B., Sharp, T. G., & Christensen, P. R. (2007). Alteration mineralogy in detachment zones: Insights from Swansea, Arizona. *Geosphere*, *3*(4), 184. https://doi.org/10.1130/GES00080.1

Michalski, J. R., Reynolds, S. J., Sharp, T. G., & Christensen, P. R. (2004). Thermal infrared analysis of weathered granitic rock compositions in the Sacaton Mountains, Arizona: Implications for petrologic classifications from thermal infrared remote-sensing data. *Journal of Geophysical Research*, *109*(3). https://doi.org/10.1029/2003je002197

Novoselov, A. A., & de Souza Filho, C. R. (2015). Potassium metasomatism of Precambrian paleosols. *Precambrian Research*, *262*, 67–83. https://doi.org/10.1016/j.precamres.2015.02.024

Nusbaum, R. L., & Grant, S. K. (1987). *Alkali metasomatism and fossil geothermal activity: Wah Wah springs tuff*. Utah: Mountain Geologist.

Roddy, M. S., Reynolds, S. J., Smith, B. M., & Ruiz, J. (1988). K-metasomatism and detachment-related mineralization, Harcuvar Mountains, Arizona. *Bulletin of the Geological Society of America*, *100*, 1627–1639. https://doi.org/10.1130/0016-7606(1988)100<1627:KMADRM>2.3.CO;2

Rogers, A. D., Bandfield, J. L., & Christensen, P. R. (2007). Global spectral classification of Martian low-albedo regions with Mars global surveyor thermal emission spectrometer (MGS-TES) data. *Journal of Geophysical Research*, *112*(E2), E02004. https://doi.org/10.1029/2006je002726

Rogers, A. D., & Nekvasil, H. (2015). Feldspathic rocks on Mars: Compositional constraints from infrared spectroscopy and possible formation mechanisms. *Geophysical Research Letters*, *42*, 2619–2626. https://doi.org/10.1002/2015GL063501

Rouchon, V., & Orberger, B. (2008). Origin and mechanisms of K-Si-metasomatism of ca. 3.4-3.3Ga volcaniclastic deposits and implications for Archean seawater evolution: Examples from cherts of Kittys Gap (Pilbara craton, Australia) and Msauli (Barberton Greenstone Belt, South Africa). *Precambrian Research*, *165*, 169–189. https://doi.org/10.1016/j.precamres.2008.06.003

Ruff, S. W., Christensen, P. R., Barbera, P. W., & Anderson, D. L. (1997). Quantitative thermal emission spectroscopy of minerals: A laboratory technique for measurement and calibration. *Journal of Geophysical Research*, *102*, 14899–14913. https://doi.org/10.1029/97jb00593

Sautter, V., Toplis, M. J., Wiens, R. C., Cousin, A., Fabre, C., Gasnault, O., et al. (2015). In situ evidence for continental crust on early Mars. *Nature Geoscience*, *8*, 605–609. https://doi.org/10.1038/ngeo2474

Smith, M. R., & Bandfield, J. L. (2012). Geology of quartz and hydrated silica-bearing deposits near Antoniadi Crater, Mars. *Journal of Geophysical Research*, *117*, E06007. https://doi.org/10.1029/2011je004038

Spencer, J. E., & Reynolds, S. J. (1986). *Geologic map of the Swansea–Copper Penny area, central Buckskin Mountains, west-central Arizona*. Tucson: ArizonaGeologicalSurvey

Spencer, J. E., Richard, S. M., Reynolds, S. J., Miller, R. J., Shafiqullah, M., Gilbert, W. G., & Grubensky, M. J. (1995). Spatial and temporal relationships between mid-Tertiary magmatism and extension in southwestern Arizona. *Journal of Geophysical Research*, *100*(B7), 10321–10351. https://doi.org/10.1029/94JB02817

Stolper, E. M., Baker, M. B., Newcombe, M. E., Schmidt, M. E., Treiman, A. H., Cousin, A., et al. (2013). The petrochemistry of Jake-M: A martian mugearite. *Science*, *341*(6153), 1239463. https://doi.org/10.1126/science.1239463

Taylor, G. J., Stopar, J. D., Boynton, W. V., Karunatillake, S., Keller, J. M., Brückner, J., et al. (2007). Variations in K/Th on Mars. *Journal of Geophysical Research*, *112*(3). https://doi.org/10.1029/2006JE002676

Thompson, L. M., Schmidt, M. E., Spray, J. G., Berger, J. A., Fairén, A. G., Campbell, J. L., et al. (2016). Potassium-rich sandstones within the Gale impact crater, Mars: The APXS perspective. *Journal of Geophysical Research: Planets*, *121*, 1981–2003. https://doi.org/10.1002/2016JE005055

Treiman, A. H., Bish, D. L., Vaniman, D. T., Chipera, S. J., Blake, D. F., Ming, D. W., et al. (2016). Mineralogy, provenance, and diagenesis of a potassic basaltic sandstone on Mars: CheMin X-ray diffraction of the Windjana sample (Kimberley area, Gale Crater). *Journal of Geophysical Research: Planets*, *121*, 75–106. https://doi.org/10.1002/2015JE004932

Wray, J. J., Hansen, S. T., Dufek, J., Swayze, G. A., Murchie, S. L., Seelos, F. P., et al. (2013). Prolonged magmatic activity on Mars inferred from the detection of felsic rocks. *Nature Geoscience*, *6*, 1013–1017. https://doi.org/10.1038/ngeo1994

Wray, J. J., Murchie, S. L., Bishop, J. L., Ehlmann, B. L., Milliken, R. E., Wilhelm, M. B., et al. (2016). Orbital evidence for more widespread carbonate-bearing rocks on Mars. *Journal of Geophysical Research: Planets*, *121*(4), 652–677. https://doi.org/10.1002/2015JE004972